CHEMISTRY OF MATERIALS

Open Access

pubs.acs.org/cm

Article

Pressure Dependence of the Second-Order Valence Phase Transition in $Eu_2Al_{15}Pt_6$ and the Solid Solutions $Eu_2Al_{15}(Pt_{5/6}T_{1/6})_6$ (T = Pd, Ir, Au)

Published as part of Chemistry of Materials special issue "Honoring the Outstanding Contributions of Mercouri Kanatzidis to Chemistry of Materials".

Lars Schumacher, Jasper A. Baldauf, Stefan Engel, Rainer Pöttgen, and Oliver Janka*

Cite This: *Chem. Mater.* 2025, 37, 10030−10035

Read Online

ACCESS | Metrics & More | Article Recommendations | Supporting Information

ABSTRACT: $Eu_2Al_{15}Pt_6$, synthesized by arc-melting, was shown to exhibit a second-order valence phase transition around 45 K, where the divalent Eu atoms get trivalent below the transition temperature T_{trans}. Substitution of Al by Ga in the solid solution $Eu_2(Al_{1-x}Ga_x)_{15}Pt_6$ leads to the vanishing of the valence phase transition at low values of x, while substitution on the Pt position, according to $Eu_2Al_{15}(Pt_{5/6}T_{1/6})_6$ with T = Pd, Ir, or Au, leads to shifts of the transition temperatures. These substitutions can be considered to superimpose either chemical or electronic pressure, leading to the question of whether the application of physical pressure also has an influence on the valence change. Pressure-dependent magnetic susceptibility measurements have been conducted on $Eu_2Al_{15}Pt_6$ and the three solid solutions $Eu_2Al_{15}(Pt_{5/6}T_{1/6})_6$ with T = Pd, Ir, and Au. In line with the expectations, the valence phase transitions under pressure occur at significantly higher temperatures, e.g., $T_{trans}(Eu_2Al_{15}Pt_6@1.0\ GPa)$ = 147(1) K, compared to ∼45 K at ambient pressure. $Eu_2Al_{15}(Pt_{5/6}Au_{1/6})_6$ does not exhibit a transition at ambient pressure, but interestingly, already at small pressures, the typical anomaly of a valence phase transition is observed in the susceptibility data.

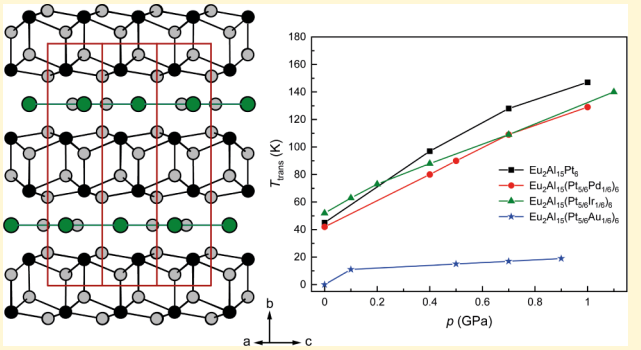

1. INTRODUCTION

Among the rare-earth elements, the trivalent oxidation state persists. However, samarium, europium, and ytterbium are known for their ability to also exhibit a divalent oxidation state besides the expected trivalent one. For Eu and Yb, the explanation is straightforward, as the divalent cations exhibit either a half-filled $4f^7$ (Eu^{2+}) or a filled $4f^{14}$ (Yb^{2+}) electron configuration. Therefore, for example, europium compounds can adopt both oxidation states, with EuO or the halides EuX_2 (X = F−I) being divalent examples,[1−3] while the Eu atoms in Eu_2O_3[4,5] or EuX_3 (X = F, Cl, Br)[6−8] are trivalent. In intermetallic compounds, usually divalent europium is observed, which is isoelectronic to Gd^{3+} and exhibits an effective magnetic moment of μ_{eff} = 7.94 μ_B, which can undergo various magnetic ordering phenomena. Examples are the pnictides $EuCd_2Pn_2$ (Pn = P, As, Sb)[9] or the large series of equiatomic EuTX phases that are summarized in a review article.[10] From a structural point of view, divalent Eu compounds exhibit a significantly larger unit cell volume in an isostructural series, e.g., $EuAl_2Pt$[11] versus $REAl_2Pt$[12] or $EuRh_2Cd_{20}$ versus $RERh_2Cd_{20}$.[13] While, as mentioned, trivalent Eu is common in the rather ionic world, trivalent intermetallic compounds are really scarce. Binary examples are $EuRh_2$,[14] $EuIr_2$,[14] $EuNi_5$,[14] Eu_2Ni_{17},[14] $EuPd_3$,[14] $EuBe_{13}$,[15] and $EuPt_5$;[14] ternary examples include $EuCo_2Si_2$,[16−19] $Eu_2Co_{12}P_7$,[20] $EuRuB_4$,[21] $EuRu_4B_4$,[21] $EuRu_2Si_2$,[17] $Eu_2Ru_3Si_5$,[22] as well as $Eu_2Al_9Ir_3$.[23] A recent review summarizes the known information on trivalent europium intermetallics alongside the typical characterization techniques.[24]

In valence phase transitions, both oxidation states are involved. In compounds exhibiting these phenomena, the valence of, e.g., Eu or Yb atoms reversibly changes from $M^{2+/3+}$ to $M^{3+/2+}$ when subjected to temperature or pressure changes. $EuAl_5Pt_3$[25] and $EuCo_2As_2$[26,27] are examples of pressure-induced valence phase transitions, while, e.g., $EuPd_2Si_2$ (T_{trans} ∼ 200 K)[28] or arc-melted $Eu_2Al_{15}Pt_6$ (T_{trans} ∼ 45 K)[29] exhibit temperature-dependent valence phase transitions. Interestingly, single crystals of $Eu_2Al_{15}Pt_6$ obtained by the Al-flux growth method show a suppression of the previously observed

Received: October 21, 2025
Revised: November 19, 2025
Accepted: November 20, 2025
Published: December 8, 2025

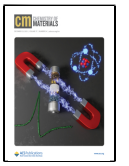

transition alongside an antiferromagnetic ground state.[30] This was traced back to a different structural ordering, as shown by single-crystal X-ray diffraction. The formation of solid solutions is readily used to manipulate the physical properties. In $Eu(Pd_{1-x}Au_x)_2Si_2$, for example, a crossover from a first- ($x = 0$) to second-order ($x = 0.15$) phase transition was observed.[31] In $Eu(Rh_{1-x}Ir_x)_2Si_2$, the stable divalent oxidation state of the Eu atoms can be shifted toward a valence-fluctuation behavior.[32] For $Eu_2Al_{15}Pt_6$ also, solid solutions have been studied. In $Eu_2(Al_{1-x}Ga_x)_{15}Pt_6$ already small amounts of Ga ($x = 0.1$) shift the Eu valence toward a stable divalent oxidation state alongside antiferromagnetic ordering.[33] This is interesting, since here an isovalent substitution of Al by Ga took place. In another solid solution, substitution was carried out on the Pt position. In $Eu_2Al_{15}(Pt_{5/6}T_{1/6})_6$ with T = Pd, Ir, and Au, the valence phase transition originally found at ∼45 K in $Eu_2Al_{15}Pt_6$ is shifted to ∼42 K upon an isovalent substitution by Pd; however, the incorporation of Ir leads to an increase of T_{trans} to 52 K.[34] This cannot only be a size effect (Ir is smaller than Pt, positive chemical pressure) but also has to have an electronic reason (negative electronic pressure, one valence electron less per sum formula). Substitution of one Pt atom by one Au atom finally leads to the disappearance of the valence phase transition, in line with a negative chemical but positive electronic pressure due to Au being larger than Pt and having an additional valence electron.

In this article, the pressure-dependent magnetic susceptibilities of polycrystalline $Eu_2Al_{15}Pt_6$ and the polycrystalline solid solutions $Eu_2Al_{15}(Pt_{5/6}T_{1/6})_6$ with T = Pd, Ir, and Au were studied. Pressures up to 1.1 GPa led to a shift of the valence phase transitions with drastically increased transition temperatures; however, at the same time, the intensity of the transition is reduced, suggesting more stable trivalent Eu atoms at elevated pressures.

2. EXPERIMENTAL SECTION

2.1. Synthesis and Characterization. All samples were prepared by arc-melting the elements as described in the respective publication for $Eu_2Al_{15}Pt_6$[29] and solid solutions $Eu_2Al_{15}(Pt_{5/6}T_{1/6})_6$[34] followed by thermal treatment to enhance the crystallinity. The obtained buttons were crushed and investigated by powder X-ray diffraction techniques, ensuring X-ray pure samples. $Eu_2Al_{15}Pt_6$ was also investigated by single-crystal X-ray diffraction techniques,[29] indicating that this compound is isostructural to $Sc_2Al_{15}Pt_6$[35] and other members of the $RE_2X_{15}Pt_6$ series (RE = Y, La−Nd, Sm, Gd−Lu; X = Al, Ga)[36] and exhibits the same modulated superstructure at room temperature. Information on the single-crystal and powder X-ray diffraction experiments, as well as SEM characterization, can be found in the respective manuscripts cited above.

2.2. Magnetic Susceptibility Measurements. The polycrystalline samples of $Eu_2Al_{15}Pt_6$ and the solid solutions $Eu_2Al_{15}(Pt_{5/6}Pd_{1/6})_6$, $Eu_2Al_{15}(Pt_{5/6}Ir_{1/6})_6$, and $Eu_2Al_{15}(Pt_{5/6}Au_{1/6})_6$ were investigated by pressure- and temperature-dependent magnetic susceptibility measurements at external fields up to 10 kOe using a Quantum Design pressure cell for magnetometry (D421).[37] The samples were ground to a fine powder and placed in a Teflon tube with a small piece of lead (HMD, Kitakyushu, Japan, about 3 mg) as a manometer for pressure calibration. Additionally, excess air was replaced by oil (Daphne 7373) as a pressure-transmitting medium. The tube was closed with two Teflon caps and centered inside a BeCu cylinder. The pressure cell was assembled, and the threads were coated in Teflon powder. The pressurization nuts were finger-tightened and placed on a sample holder rod of a Dynacool physical property measurement system (PPMS) using the vibrating sample magnetometer (VSM) option.

The pressure cell was cooled to 6 K. A small external magnetic field between −20 and 20 Oe was applied to the sample in order to achieve a magnetization between -1×10^{-4} and -1×10^{-5} emu. The temperature was then set to 7.5 at 0.1 K min^{-1} and the temperature-dependent magnetization data was collected. The critical temperature of lead was determined at the maximum slope of the transition and used as a reference for ambient pressure. The transition temperature of lead is pressure sensitive and can be approximated using the following formula (eq 1):

$$\frac{dT_c}{dP}(\mathrm{K\ GPa^{-1}}) = -0.379\ \mathrm{K\ GPa^{-1}} \quad (1)$$

The cell was afterward tightened equally on both sides for 0.1 to 0.3 mm each, and the critical temperature was again determined the same way. With the shift of the critical temperature and eq 1, the pressure inside the cell could be determined. With the precision of the temperature determination from $d\chi/dT$ being between 0.01 and 0.03 K, the resulting error on the pressure is between 0.03 and 0.07 GPa. A maximum compression of about 1 mm was targeted to avoid damaging the cell. For each pressure, zero-field-cooled data at 10 kOe could be measured using an amplitude of 1 mm and a frequency of 40 Hz.

3. RESULTS

3.1. Crystal Chemistry. Initially, in 2002, the compound with the nominal composition $Gd_{0.67}Al_5Pt_2$[38] was reported to crystallize in the hexagonal $Sc_{0.6}Fe_2Si_{4.9}$ type structure[39] with space group $P6_3/mmc$. Later, in 2004, Niermann and Jeitschko reported more members; however, they used the sum formula $M_2Al_{15}Pt_6$ with M = Y, Gd−Tm, Zr.[40] The reason being that some of the refined atomic positions were only partially occupied and that diffuse reflections were observed that would justify a $\sqrt{3} \times \sqrt{3}$ enlarged unit cell. Prots and coworkers were able to refine the crystal structure of $Yb_2Al_{15}Pt_6$ in the orthorhombic crystal system with space group $Cmcm$[41] while Radzieowski et al. refined the crystal structure of $Sc_2Al_{15}Pt_6$ as a (3+1)D modulated structure ($q = (2/3a^*,0,0)$) with a monoclinic approximant.[35] Later, the same modulated structure was also observed for $Eu_2Al_{15}Pt_6$[29] and $Ho_2Al_{15}Pt_6$.[36] Recently, the solution growth of $Eu_2Al_{15}Pt_6$ was described, leading to large single crystals that were subject to single-crystal X-ray diffraction.[30] Interestingly, the observed diffraction patterns differed quite significantly from those of arc-melted $Eu_2Al_{15}Pt_6$. Although the structure could not satisfactorily be refined due to the complex nature of the

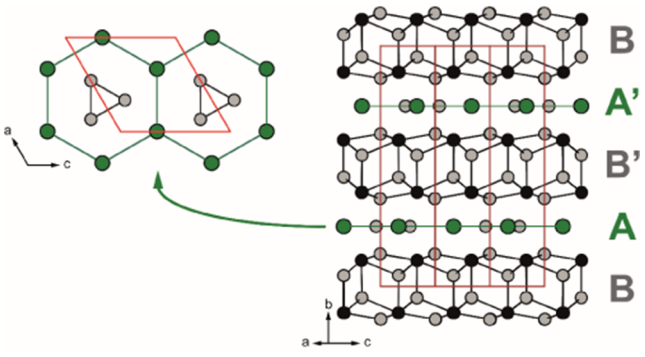

Figure 1. (*right*) Unit cell of the monoclinic approximant of $Eu_2Al_{15}Pt_6$. Bonds between the layers have been omitted for clarity; (*left*) layer formed by the Eu atoms and the Al_3 triangles. Eu atoms are depicted in green, Al atoms in gray, and Pt atoms in black, respectively.

https://doi.org/10.1021/acs.chemmater.5c02813
Chem. Mater. 2025, 37, 10030−10035

Table 1. Lattice Parameters and Unit Cell Volumes of $Eu_2Al_{15}Pt_6$, $Eu_2Al_{15}(Pt_{5/6}Pd_{1/6})_6$, $Eu_2Al_{15}(Pt_{5/6}Ir_{1/6})_6$, and $Eu_2Al_{15}(Pt_{5/6}Au_{1/6})_6$ Determined by Powder X-ray Diffraction[a]

Compound	a(pm)	c(pm)	V (nm^3)	Ref.
$Eu_2Al_{15}Pt_6$	429.47(2)	1666.7(2)	0.2652	29
$Eu_2Al_{15}(Pt_{5/6}Pd_{1/6})_6$	429.55(1)	1665.9(2)	0.2662	34
$Eu_2Al_{15}(Pt_{5/6}Ir_{1/6})_6$	429.38(1)	1666.2(2)	0.2660	34
$Eu_2Al_{15}(Pt_{5/6}Au_{1/6})_6$	430.32(1)	1665.8(3)	0.2671	34

[a]The lattice parameters of the average hexagonal structure ($Sc_{0.6}Fe_2Si_{4.9}$ type, $P6_3/mmc$[39]) are given.

modulation, a different stacking of the Al_3 triangle-centered Eu layers could be deduced.

As the crystal structure of $Eu_2Al_{15}Pt_6$ and its related compounds has been described in detail before,[29,35,36] only the important structural features will be highlighted. The structure (Figure 1) can be described by two building blocks: [Pt_3Al_6] slabs (block B) and planar layers of Eu atoms, arranged in a honeycomb pattern, that are centered by Al_3 triangles (block A). The latter are responsible for the interesting magnetic properties of $Eu_2Al_{15}Pt_6$. These are alternatingly stacked along the crystallographic b-axis (monoclinic setting) in an ···ABA′B′··· sequence. Bonding interactions are also observed between the layers; however, these

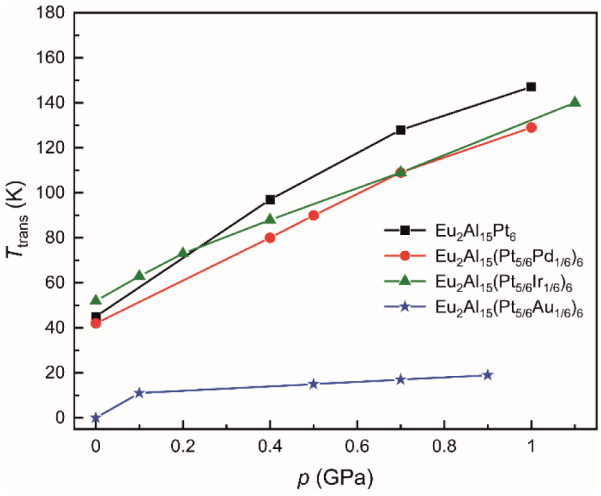

Figure 3. Temperature of the second-order valence phase transition of $Eu_2Al_{15}Pt_6$ (black), $Eu_2Al_{15}(Pt_{5/6}Pd_{1/6})_6$ (red), $Eu_2Al_{15}(Pt_{5/6}Ir_{1/6})_6$ (green), and $Eu_2Al_{15}(Pt_{5/6}Au_{1/6})_6$ (blue) plotted against the applied physical pressure.

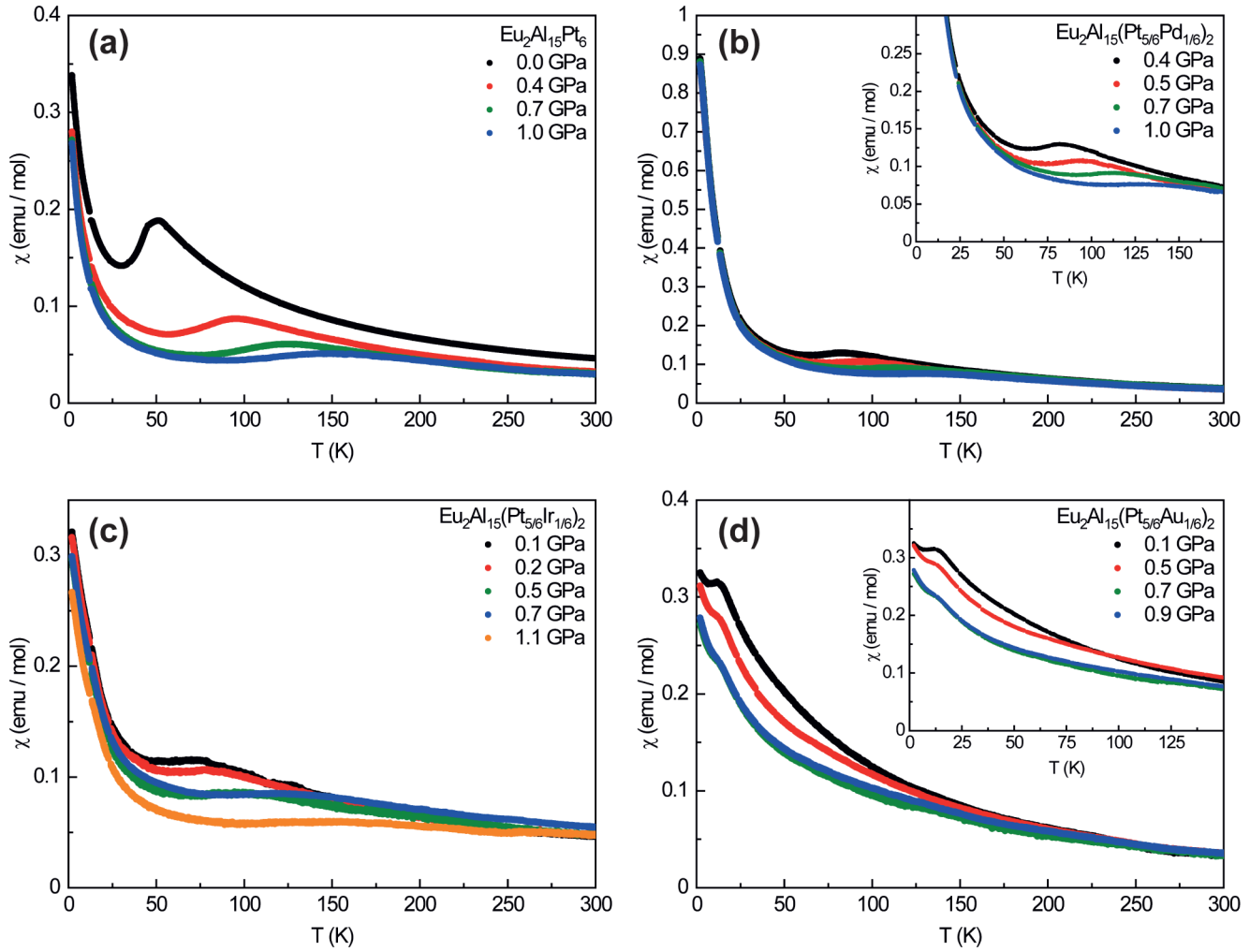

Figure 2. Temperature-dependent magnetic susceptibility of (a) $Eu_2Al_{15}Pt_6$, (b) $Eu_2Al_{15}(Pt_{5/6}Pd_{1/6})_6$, (c) $Eu_2Al_{15}(Pt_{5/6}Ir_{1/6})_6$, and (d) $Eu_2Al_{15}(Pt_{5/6}Au_{1/6})_6$ measured at different pressures. Where necessary, the inset shows the zoomed low-temperature regime.

https://doi.org/10.1021/acs.chemmater.5c02813
Chem. Mater. 2025, 37, 10030−10035

are omitted in Figure 1 for better visibility of the fundamental building blocks. Additional details can be found in the literature.[29,35,36]

For the solid solutions $Eu_2Al_{15}(Pt_{5/6}T_{1/6})_6$ with T = Pd, Ir, and Au, only powder X-ray diffraction data was collected. Due to the nature of the modulated structure, the superstructure reflections of the monoclinic unit cell are not observable in the powder data; therefore, the unit cell parameters were refined in the average hexagonal structure (Table 1).

3.2. Magnetic Measurements. $Eu_2Al_{15}Pt_6$ exhibits a temperature-dependent second-order valence phase transition around $T_{trans} \sim 45$ K, where the divalent Eu atoms delocalize an electron, forming Eu^{3+}, presumably due to the thermal contraction of the crystal structure. This valence phase transition has been characterized in detail by magnetic, resistivity, and heat capacity measurements, as well as ^{151}Eu Mössbauer spectroscopic investigations.[29] Investigations of the solid solution $Eu_2(Al_{1-x}Ga_x)_{15}Pt_6$ indicated a shift toward lower temperatures for $x = 0.05$, while for $x = 0.1$, the valence phase transition is suppressed. With even higher degrees of substitution, an antiferromagnetic transition, as reported for $Eu_2Ga_{15}Pt_6$, emerges.[33] As the substitution of Al with Ga suppresses the valence phase transition quite effectively, three solid solutions substituting Pt for neighboring transition metals have been investigated. It was shown that formally only one out of the six Pt atoms can be substituted by Pd, Ir, or Au; however, no structural ordering is observed. For $Eu_2Al_{15}(Pt_{5/6}Pd_{1/6})_6$, only a slight shift of the transition temperature is observed, while for $Eu_2Al_{15}(Pt_{5/6}Au_{1/6})_6$, the transition fully vanishes. For $Eu_2Al_{15}(Pt_{5/6}Ir_{1/6})_6$, an increase to $T_{trans} \sim 52$ K was observed. This behavior was attributed to the combination of electronic and size effects.

Temperature-dependent magnetic susceptibility measurements were conducted at different pressures. Figure 2a shows the magnetic susceptibilities of $Eu_2Al_{15}Pt_6$ measured at 0, 0.4, 0.7, and 1.0 GPa. It is clearly evident that the valence phase transition shifts to higher temperatures while at the same time significantly losing in intensity. This shows that the formal intrinsic oxidation ($Eu^{2+} \rightarrow Eu^{3+}$) under a physical pressure happens at significantly higher temperatures. This is in line with the observations made for $Eu_2Al_{15}(Pt_{5/6}Ir_{1/6})_6$. Here the smaller Ir atoms cause a contraction of the structure due to "chemical pressure". The overall flattening of the susceptibility trace can be explained by the destabilization of the divalent oxidation state. For $Eu_2Al_{15}(Pt_{5/6}Pd_{1/6})_6$ (Figure 2b) a very similar trend is observed. Here, however, the effect is already dampened, even before applying physical pressure. For $Eu_2Al_{15}(Pt_{5/6}Ir_{1/6})_6$ the same shift is observed (Figure 2c); here, however, the effect has almost vanished at 1.1 GPa. Finally, $Eu_2Al_{15}(Pt_{5/6}Au_{1/6})_6$ was quite surprising, as this solid solution shows no observable valence phase transition at ambient pressure (Figure 2d). However, by applying as little as 0.1 GPa, a shoulder similar to prototypic $Eu_2Al_{15}Pt_6$ emerges. Higher pressures shift this shoulder only slightly. Figure 3 shows a comparison of the extracted temperatures at which the valence phase transitions occur for the different compounds. Here a clear increase is visible for $Eu_2Al_{15}Pt_6$, $Eu_2Al_{15}(Pt_{5/6}Pd_{1/6})_6$, and $Eu_2Al_{15}(Pt_{5/6}Ir_{1/6})_6$, all showing a very similar slope, while for $Eu_2Al_{15}(Pt_{5/6}Au_{1/6})_6$, only a very small increase in the transition temperature is visible.

Looking at the normal pressure and high-pressure data, one can try to explain the observations as follows: decreasing the temperature leads to contractions of the unit cells of all of the investigated compounds. The valence phase transition happens at a temperature where the divalent oxidation state of the Eu atoms is destabilized enough so an intrinsic oxidation alongside a delocalization of an electron takes place, leading to trivalent Eu atoms. A similar effect takes place when pressure is applied. The unit cell is contracted; however, the applied pressures are, in all cases, not high enough so that the valence phase transition happens only when pressure induced. But due to the precontraction of the cell, the transition temperature shifts to higher values.

4. CONCLUSION

The temperature dependence of the second-order valence phase transition of $Eu_2Al_{15}Pt_6$ and the solid solutions $Eu_2Al_{15}(Pt_{5/6}Pd_{1/6})_6$, $Eu_2Al_{15}(Pt_{5/6}Ir_{1/6})_6$, and $Eu_2Al_{15}(Pt_{5/6}Au_{1/6})_6$ was studied by magnetic susceptibility measurements at different applied pressures. It is clearly visible that the transition temperature increases with increasing pressure while at the same time losing in intensity. This suggests that the intrinsic oxidation from Eu^{2+} to Eu^{3+} happens at higher temperatures along with a destabilization of the divalent oxidation state. Surprisingly, this valence phase transition also occurs for $Eu_2Al_{15}(Pt_{5/6}Au_{1/6})_6$ under elevated pressures above 0.1 GPa since it is not visible at ambient pressure.

■ ASSOCIATED CONTENT

Data Availability Statement

The data that support the findings of this study are available from the corresponding author upon reasonable request.

Supporting Information

The Supporting Information is available free of charge at https://pubs.acs.org/doi/10.1021/acs.chemmater.5c02813.

Pressure calibration curves for magnetic susceptibility measurements (PDF)

■ AUTHOR INFORMATION

Corresponding Author

Oliver Janka − *Inorganic Solid State Chemistry, Saarland University, Saarbrücken 66123, Germany;* orcid.org/0000-0002-9480-3888; Email: oliver.janka@uni-saarland.de

Authors

Lars Schumacher − *Institut für Anorganische und Analytische Chemie, Universität Münster, Münster 48149, Germany;* orcid.org/0009-0009-9444-8773

Jasper A. Baldauf − *Institut für Anorganische und Analytische Chemie, Universität Münster, Münster 48149, Germany;* orcid.org/0009-0004-8187-0864

Stefan Engel − *Inorganic Solid State Chemistry, Saarland University, Saarbrücken 66123, Germany;* orcid.org/0000-0002-6813-8490

Rainer Pöttgen − *Institut für Anorganische und Analytische Chemie, Universität Münster, Münster 48149, Germany;* orcid.org/0000-0003-0962-279X

Complete contact information is available at: https://pubs.acs.org/10.1021/acs.chemmater.5c02813

Author Contributions

All authors have accepted responsibility for the entire content of this submitted manuscript and approved the submission.

Funding

Funding is provided by Universität Münster and Deutsche Forschungsgemeinschaft (DFG) (JA 1891-10-1 and INST 211/1034-1).

Notes

The authors declare no competing financial interest.

REFERENCES

(1) Szytuła, A.; Leciejewicz, J. *Handbook Of Crystal Structures And Magnetic Properties Of Rare Earth Intermetallics*; CRC Press: Boca Raton, 1994.
(2) Emsley, J.; *The Elements*; Clarendon Press: New York, 1998.
(3) Cotton, S. *Lanthanides and Actinide*; Red Globe Press: London, 1991.
(4) Zachariasen, W. H. The crystal structure of the modification C of the sesquioxides of the rare earth metals, and of indium and thallium. *Nor. Geol. Tidsskr.* **1927**, *9*, 310−316.
(5) Zachariasen, W. H. Untersuchungen über die Kristallstruktur von Sesquioxyden und Verbindungen ABO_3. *Skr. Nor. Vidensk.-Akad.* **1929**, *4*, 1−166.
(6) Zalkin, A.; Templeton, D. H. The crystal structures of YF_3 and related compounds. *J. Am. Chem. Soc.* **1953**, *75*, 2453−2458.
(7) Templeton, D. H.; Dauben, C. H. Lattice parameters of some rare earth compounds and a set of crystal radii. *J. Am. Chem. Soc.* **1954**, *76*, 5237−5239.
(8) Lyle, S. J.; Westall, W. A. A study of an anhydrous europium bromide mixed-valence phase. *J. Less-Common Met.* **1985**, *106*, 109−116.
(9) Schellenberg, I.; Pfannenschmidt, U.; Eul, M.; Schwickert, C.; Pöttgen, R. A ^{121}Sb and ^{151}Eu Mössbauer Spectroscopic Investigation of $EuCd_2X_2$ (X = P, As, Sb) and $YbCd_2Sb_2$. *Z. Anorg. Allg. Chem.* **2011**, *637*, 1863−1870.
(10) Pöttgen, R.; Johrendt, D. Equiatomic intermetallic europium compounds: syntheses, crystal chemistry, chemical bonding, and physical properties. *Chem. Mater.* **2000**, *12*, 875−897.
(11) Stegemann, F.; Block, T.; Klenner, S.; Zhang, Y.; Fokwa, B. P. T.; Timmer, A.; Mönig, H.; Doerenkamp, C.; Eckert, H.; Janka, O. From 3D to 2D: structural, spectroscopical and theoretical investigations of the dimensionality reduction in the $[PtAl_2]^{\delta-}$ polyanions of the isotypic $MPtAl_2$ series (M = Ca−Ba, Eu). *Chem. Eur. J.* **2019**, *25*, 10735−10747.
(12) Radzieowski, M.; Stegemann, F.; Doerenkamp, C.; Matar, S. F.; Eckert, H.; Dosche, C.; Wittstock, G.; Janka, O. Correlations of crystal and electronic structure via NMR and XPS spectroscopy in the $RETMAl_2$ (RE = Sc, Y, La−Nd, Sm, Gd−Tm, Lu; TM = Ni, Pd, Pt) series. *Inorg. Chem.* **2019**, *58*, 7010−7025.
(13) Schumacher, L.; Schreiner, F.; Koldemir, A.; Janka, O.; Hansen, M. R.; Pöttgen, R. Cadmium-rich intermetallic phases ARh_2Cd_{20} − structure, magnetic behavior, ^{151}Eu Mössbauer and ^{113}Cd solid-state NMR spectroscopy. *Dalton Trans.* **2025**, *54*, 8100−8112.
(14) De Vries, J. W. C.; Thiel, R. C.; Buschow, K. H. J. The ^{151}Eu Mössbauer isomer shift in intermetallic compounds containing trivalent europium. *Physica B+C* **1984**, *124* (3), 291−298.
(15) Hidaka, H.; Mizuuchi, K.; Yanagisawa, T.; Amitsuka, H. Magnetic, Transport, and Phonon Properties of the Trivalent Eu Metallic Compound $EuBe_{13}$. *J. Phys. Soc. Jpn.* **2019**, *88* (3), 034708.
(16) Seiro, S.; Kummer, K.; Vyalikh, D.; Caroca-Canales, N.; Geibel, C. Anomalous susceptibility in single crystals of $EuCo_2Si_2$ with trivalent Eu: Influence of excited J multiplets. *Phys. Status Solidi B* **2013**, *250*, 621−625.
(17) Felner, I.; Nowik, I. Itinerant and local magnetism, superconductivity and mixed valency phenomena in RM_2Si_2, (R = rare earth, M = Rh, Ru). *J. Phys. Chem. Solids* **1984**, *45*, 419−426.
(18) Mayer, I.; Felner, I. Europium silicides and germanides of the EuM_2X_2 type: Crystal structure and the valence states of europium. *J. Phys. Chem. Solids* **1977**, *38*, 1031−1034.
(19) Maślankiewicz, P.; Szade, J. Valence instability of europium in $EuCo_2Si_2$. *J. Alloys Compd.* **2006**, *423*, 69−73.
(20) Mörsen, E.; Mosel, B. D.; Müller-Warmuth, W.; Reehuis, M.; Jeitschko, W. A ^{151}Eu Mössbauer study of the magnetic hyperfine interactions in the metallic compound $Eu_2Co_{12}P_7$ containing trivalent europium. *J. Phys. C: Solid State Phys.* **1988**, *21*, 3133−3140.
(21) Harmening, T.; Pöttgen, R. ^{151}Eu Mössbauer spectroscopic characterization of $EuRu_4B_4$ and the new boride $EuRuB_4$. *Z. Naturforsch. B* **2010**, *65*, 90−94.
(22) Seidel, S.; Harmening, T.; Kösters, J.; Koldemir, A.; Pröbsting, W.; Engelbert, S.; Pöttgen, R. $Eu_2Ru_3Si_5$ and $Eu_2Ir_3Ga_5$ − first europium compounds with $U_2Mn_3Si_5$-type structure but different europium valence. *Z. Naturforsch. B* **2023**, *78*, 293−300.
(23) Stegemann, F.; Block, T.; Klenner, S.; Janka, O. An unusual valence state: trivalent europium in intermetallic $Eu_2Ir_3Al_9$. *Chem. A Eur. J.* **2019**, *25* (14), 3505−3509.
(24) Engel, S.; Gießelmann, E. C. J.; Pöttgen, R.; Janka, O. Trivalent europium − a scarce case in intermetallics. *Rev. Inorg. Chem.* **2023**, *43*, 571−582.
(25) Koizumi, T.; Honda, F.; Sato, Y. J.; Li, D.; Aoki, D.; Haga, Y.; Gouchi, J.; Nagasaki, S.; Uwatoko, Y.; Kaneko, Y.; Ōnuki, Y. Abrupt change in electronic states under pressure in new compound $EuPt_3Al_5$. *J. Phys. Soc. Jpn.* **2022**, *91*, 043704.
(26) Menushenkov, A. P.; Yaroslavtsev, A. A.; Geondzhian, A. Y.; Chernikov, R. V.; Nataf, L.; Tan, X.; Shatruk, M. Driving the europium valence state in $EuCo_2As_2$ by external and internal impact. *J. Supercond. Novel Magn.* **2017**, *30*, 75−78.
(27) Tan, X.; Fabbris, G.; Haskel, D.; Yaroslavtsev, A. A.; Cao, H.; Thompson, C. M.; Kovnir, K.; Menushenkov, A. P.; Chernikov, R. V.; Garlea, V. O.; Shatruk, M. A transition from localized to strongly correlated electron behavior and mixed valence driven by physical or chemical pressure in ACo_2As_2 (A = Eu and Ca). *J. Am. Chem. Soc.* **2016**, *138*, 2724−2731.
(28) Sampathkumaran, E. V.; Gupta, L. C.; Vijayaraghavan, R.; Gopalakrishnan, K. V.; Pillay, R. G.; Devare, H. G. A new and unique Eu-based mixed valence system: $EuPd_2Si_2$. *J. Phys. C: Solid State Phys.* **1981**, *14*, L237−L241.
(29) Radzieowski, M.; Stegemann, F.; Block, T.; Stahl, J.; Johrendt, D.; Janka, O. Abrupt europium valence change in $Eu_2Pt_6Al_{15}$ around 45 K. *J. Am. Chem. Soc.* **2018**, *140*, 8950−8957.
(30) Schmidt, J.; Ryan, D. H.; Janka, O.; Kösters, J.; Mueller, C. L.; Sapkota, A.; Penacchio, R. F. S.; Slade, T. J.; Bud'ko, S. L.; Canfield, P. C. Suppression of the valence transition in solution-grown single crystals of $Eu_2Pt_6Al_{15}$. *Phys. Rev. Mater.* **2025**, *9* (9), 093404.
(31) Abd-Elmeguid, M. M.; Sauer, C.; Köbler, U.; Zinn, W.; Röhler, J.; Keulerz, K. Valence instability in magnetically ordered $Eu(Pd_{1-x}Au_x)_2Si_2$. *J. Magn. Magn. Mater.* **1985**, *47*−*48*, 417−419.
(32) Seiro, S.; Geibel, C. From stable divalent to valence-fluctuating behaviour in $Eu(Rh_{1-x}Ir_x)_2Si_2$ single crystals. *J. Phys.: Condens. Matter.* **2011**, *23*, 375601.
(33) Oyama, K.; Mitsuda, A.; Wada, H.; Narumi, Y.; Hagiwara, M.; Takahashi, R.; Wadati, H.; Setoyama, H.; Kindo, K. Ga substitution effect on the valence transition of $Eu_2Pt_6Al_{15}$. *J. Phys. Soc. Jpn.* **2020**, *89*, 114713.
(34) Engel, S.; Schumacher, L.; Janka, O. Modifying the valence phase transition in $Eu_2Al_{15}Pt_6$ by the solid solutions $Eu_2Al_{15}(Pt_{1-x}T_x)_6$ (T = Pd, Ir, Au; x = 1/6). *Z. Naturforsch. B* **2024**, *79b*, 21−27.
(35) Radzieowski, M.; Stegemann, F.; Hoffmann, R.-D.; Janka, O. The monoclinic superstructure of the $M_2Pt_6Al_{15}$ series (M = Ca, Sc, Y, La, Lu). *Z. Kristallogr. Cryst. Mater.* **2017**, *232*, 675−687.
(36) Radzieowski, M.; Stegemann, F.; Janka, O. Magnetic properties of the $RE_2Pt_6X_{15}$ (RE = Y, La−Nd, Sm, Gd−Lu; X = Al, Ga) Series. *Eur. J. Inorg. Chem.* **2020**, *2020*, 1199−1210.
(37) Quantum Design. *High Pressure Cell User Manual*; Quantum Design: Japan, 2016.
(38) Latturner, S. E.; Kanatzidis, M. G. $Gd_{1.33}Pt_3(Al,Si)_8$ and $Gd_{0.67}Pt_2(Al,Si)_5$: two structures containing a disordered Gd/Al layer grown in liquid aluminum. *Inorg. Chem.* **2002**, *41*, 5479−5486.
(39) Kotur, B.; Bruvo, M.; Kirsch, S. G. Crystal structure of the silicide $Sc_{1.2}Fe_4Si_{9.8}$. *Sov. Phys. Crystallogr.* **1991**, *36*, 787−789.

https://doi.org/10.1021/acs.chemmater.5c02813
Chem. Mater. 2025, 37, 10030−10035

(40) Niermann, J.; Jeitschko, W. Ternary aluminides with the ideal composition $A_2Pt_6Al_{15}$ (A = Y, Gd−Tm, Zr). *Z. Anorg. Allg. Chem.* **2004**, *630*, 361−368.
(41) Prots, Y.; Deppe, M.; Cardoso Gil, R. H.; Cervellino, A.; Ormeci, A.; Geibel, C.; Grin, Y. $Yb_2Al_{15}Pt_6$ - the most ordered variety of the $Sc_{1.2}Fe_4Si_{9.8}$ aristotype. *Chem. Met. Alloys* **2014**, *7*, 85−99.

https://doi.org/10.1021/acs.chemmater.5c02813
Chem. Mater. 2025, 37, 10030−10035